Available online at www.sciencedirect.com

ScienceDirect

Ceramics International 39 (2013) 9671–9675

CERAMICS INTERNATIONAL

www.elsevier.com/locate/ceramint

Synthesis and characterization of WC—VC—Co nanocomposite powders through thermal-processing of a core—shell precursor

Hua Lin[a,b,*], Bo-Wan Tao[a], Jie Xiong[a], Qing Li[b]

[a]State Key Laboratory of Electronic Thin Films and Integrated Devices, University of Electronic Science and Technology of China, Chengdu 610054, PR China
[b]School of Materials Science and Engineering, Southwest University, Chongqing 400715, PR China

Received 13 March 2013; received in revised form 23 May 2013; accepted 23 May 2013
Available online 4 June 2013

Abstract

WC—VC—Co nanocomposite powders were synthesized through simultaneous reduction and carburization of a novel precursor in vacuum at 950 °C for 1 h. The samples were characterized by X-ray diffraction, scanning electron microscopy, transmission electron microscopy, high-resolution transmission electron microscopy, and X-ray photoelectron spectroscopy. The precursor consisted of nanoparticles (from 10 nm to 30 nm in diameter) with a carbon-coated core—shell structure. The as-prepared composite powders comprised spherical particles with size in the range of 40—60 nm. The effects of experimental parameters and reaction mechanism were explored. The low-temperature synthesis and short reaction time were attributed to the homogeneous chemical composition of the precursor.

Keywords: A. Power processing; B. Nanocomposites; B. X-ray diffraction; E. Ceramics.

1. Introduction

WC—Co cemented carbides are widely used as materials for machining tools, mining tools, and wear-resistant parts because of their high strength, hardness, and good wear resistance [1]. Their application has faced huge challenges with the development of high-precision industries [2]. The traditional carbide does not satisfy the requirements of electronics, medicine, aerospace, and other industries that necessitate high strength, hardness, and prolonged carbide lifespan [3—5]. Studies have shown that the reduction of crystalline size of cermet could remarkably improve mechanical properties [6,7]. Hence, the preparation of nanometer-sized WC—Co cemented carbides has recently received increasing attention.

Numerous methods have been used to synthesize ultrafine and nano-cermet [8—11]. However, the abnormal grain growth of nanocrystalline cermet during liquid-phase sintering remains as a common problem [12]. To date, the most effective method to control the growth of WC—Co grain is by adding grain-growth inhibitors, such as VC, Cr_3C_2, NbC, or TaC, into the starting powder mixtures [12—15]. Such grain growth inhibitors have exhibited the following roles: (1) inhibitors absorbed on the surface of carbide particles could reduce the surface energy of WC, thereby preventing recrystallization through liquid; and (2) the common ion effect of C could prevent the dissolution of WC at the Co melting point [16,17].

Improvements in the mechanical properties of hard alloys depend on the grain size reduction, addition of grain-growth inhibitors, and the improvement of other qualities (cleanness, homogeneity, and grain size distribution) of the powders. The starting quality of powders requires careful attention to enable the use of ceramics in advanced practical applications. Most methods in preparing WC—VC—Co composite powders involve the following steps: (1) WC, VC, and Co are produced from metals or metal oxides through reduction and carbonization; and (2) the final WC—VC—Co composite powers are formed through mechanical milling of WC, VC and Co powders for a certain period of time during which a lubricant is added to aid in the subsequent pressing [12,14,18,19]. These processes encounter problems such as the introduction of impurities and heterogeneous mixing. An ideal solution to

*Corresponding author at: State Key Laboratory of Electronic Thin Films and Integrated Devices, University of Electronic Science and Technology of China, Chengdu 610054, PR China. Tel./fax: +86 28 83201232.
E-mail address: lh2004@swu.edu.cn (H. Lin).

0272-8842/$ - see front matter © 2013 Elsevier Ltd and Techna Group S.r.l. All rights reserved.
http://dx.doi.org/10.1016/j.ceramint.2013.05.092

this problem is the single-step preparation of WC—VC—Co nanocomposite powders described in Ref. [14], but this method is expensive and difficult to control.

The development of an inexpensive and facile direct method is thus necessary to synthesize pure and uniform components. In our previous study, we demonstrated an effective means to prepare composite powders using a core—shell structured precursor [20]. In the current paper, a similar method was adopted to prepare the precursor. The core was a W, Co, and V compound with a C shell. The WC—VC—Co nanocomposite powders were synthesized from the precursor without the use of expensive reductive gas or complex equipment by in situ reduction and carburization in vacuum. To date, this method has not been developed for post-synthesis or extensively reported in literature.

2. Experiments

Commercial ammonium metatungstate {AMT[$(NH_4)6(H_2W_{12}O_{40})\cdot 4H_2O$]}, ammonium metavanadate (NH_4VO_3), cobalt chloride ($CoCl_2\cdot 6H_2O$), and soluble starch $(C_6H_{10}O_5)$n (molecular weight: 342.29) purchased from Chendu Kelong Chemical plant were used as the sources of W, V, Co and C, respectively. All reagents used were of analytical grade.

$CoCl_2\cdot 6H_2O$ (0.96 g) and $(C_6H_{10}O_5)$n (2.69 g) were combined and dissolved in 20 ml deionized water to form a transparent amaranthine solution. AMT (1.17 g) and NH_4VO_3 (0.54 g) were dissolved in 20 ml deionized water at 60 °C under vigorous stirring. The two solutions were mixed in a 100 ml Teflon-lined autoclave. The autoclave was sealed in a stainless steel tank and maintained at 200 °C for 10 h without shaking or stirring. After autoclaving, the product was naturally cooled to room temperature and diluted with 100 ml deionized water to form a suspension. Brown precursor powders were then obtained by spray-drying the suspension at a feeding rate of 25 ml min^{-1} under 250 °C hot air. Finally, the target products were obtained by heating the precursor powders in a vacuum furnace at 950 °C at an increment of 10 K min^{-1} and held for 1 h.

The phase was identified using an X-ray diffractometer (XD-3, Purkinje, Beijing) with Cu Kα radiation ($\lambda=0.15406$ nm) at a scanning rate of 0.02°/s in the 2θ range of 30—88°. Scanning electron microscopy (SEM) images were taken using a Hitachi S-4800 field emission scanning electron microscope. High-resolution transmission electron microscopy (HRTEM) images were obtained with an FEI Tecnai-G2F20 using an accelerating voltage of 200 kV. The X-ray photoelectron spectroscopy (XPS) spectra were recorded with an XSAM 800 photoelectron spectrometer (Kratos, England) using non-monochromatized Mg Kα ($\lambda=0.9889$ nm) X-ray as the excitation source.

To measure the amount of residual metal ions, the original solution after hydrothermal processing was filtered. The filtrate liquor was titrated using 0.1 mol L^{-1} HNO_3 and then stood for 24 h. The precipitation was collected by centrifugal separation, washed with distilled water and ethanol several times, and dried in vacuum at 60 °C for 4 h. Based on the weight of the precipitation, the amount of residual ions can be calculated. The principle of the measurement method is in accordance with a method reported by Supothina et al. [21].

3. Results and discussion

During the hydrothermal process, the metallic compounds were decomposed and then reunited to form nanoparticle nucleates with an increase in temperature. The crucial parameters were the reaction temperature and holding time, and their influence was explored. In our proposed method, increasing the temperature accelerated the reaction. When the temperature was lower than 180 °C, only a small amount of precipitate was obtained even after 12 h, indicating a very low nanoparticle nucleation rate. When the temperature was higher than 220 °C, the carbonization process was severe, and several graphite spheres were generated. Thus, 200 °C was selected as the base temperature. Adjusting the holding time was found to enable manipulation of the amount of metal ions to form a core. The amount of residual metal ions decreased with prolonged hydrothermal time (Fig. 1). When the holding time was prolonged to 8, 10, and 12 h, the amounts of residual metal ions were 5.6%, 0.8%, and 0.6%, respectively. A small amount of residual metal ions did not affect the preparation of the composite powders. The residual metal ions were evenly deposited on the surface of the core—shell particles to obtain a uniform precursor during the spray-drying process.

A transmission electron microscopy (TEM) image of the precursor particles prepared at 200 °C for 10 h is shown in Fig. 2. The particles have typical core—shell structures and assume spherical shapes with approximately 10—30 nm diameter with an even dispersion. To obtain a more detailed sample structure, HRTEM measurement was performed on the interface of a randomly chosen core—shell structure (inset of Fig. 2). The interface of the core and shell was evidently observed at different orientations, indicating a typical core—shell structure.

The X-ray diffraction (XRD) patterns of the products prepared under different temperatures are shown in Fig. 3. The η phase, such as CCo_2W_4, W_2C, and W, was easily generated at 850 °C (Fig. 3a). After heating at 900 °C, the

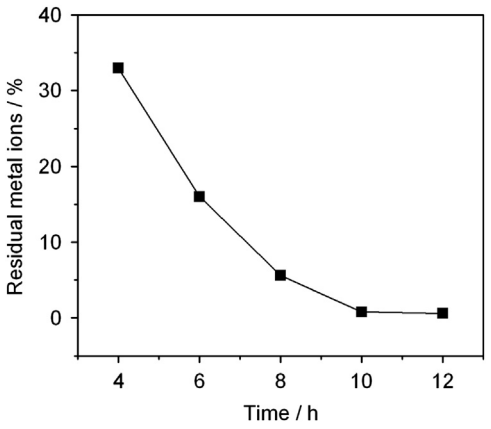

Fig. 1. Function of the amount of residual metal ions versus hydrothermal time.

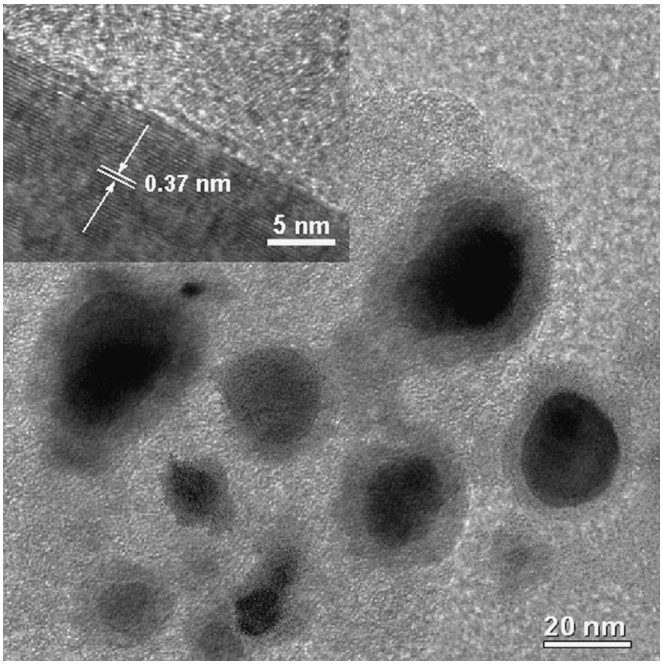

Fig. 2. TEM image of the as-prepared precursor (inset is the interface of a randomly chosen precursor particle).

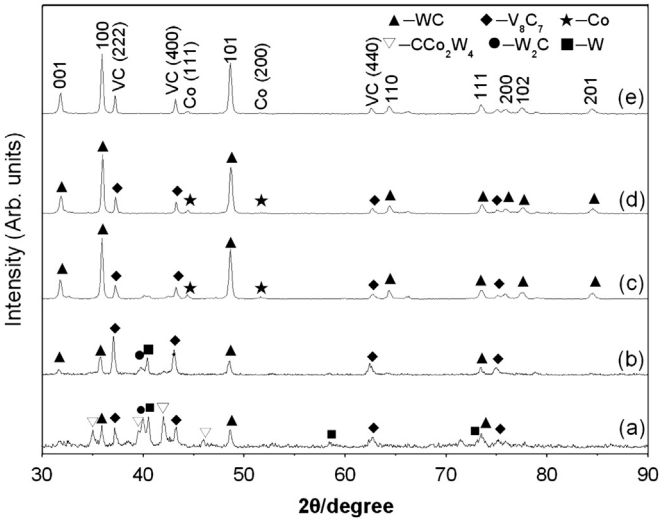

Fig. 3. XRD patterns of the samples prepared at (a) 850 °C, 1 h; (b) 900 °C, 1 h; (c) 950 °C, 1 h; (d) 1000 °C, 1 h; and (e) 1200 °C, 2 h.

diffraction peaks of V_8C_7 and WC became noticeable, indicating that the products had been generated (Fig. 3b). In addition, a small amount of W_2C and W, but no peak of Co, was detected. When the reaction temperature was increased to 950 °C (Fig. 3c), the peaks could be indexed as closely packed hexagonal-structured WC (JCPDS 89-2727), face-centered cubic structured Co (JCPDS 89-4307), and face-centered cubic structured V_8C_7 (JCPDS 73-0394). No peak of the η phase was observed. Considered as a catalyst in WC formation [5], Co was not observed before 950 °C. At this point, the reaction is over and the Co crystallized and recovered its original character. The intensity of the diffraction peaks of V_8C_7 is stronger than that of Co, which absorbed the X-ray from copper. To investigate the product stability, the precursor was treated at 1000 °C for 1 h and at 1200 °C for 2 h and the results are shown in Fig. 3d and e, respectively. Compared with the corresponding lines in Fig. 3c, the peaks did not change with increased temperatures and prolonged holding times. No metallic W or other C-deficient W carbides were generated. This result differs from the previous one where the product was prepared in a CH_4—H_2 atmosphere [21]. The gases CH_4 and H_2 may have reacted with WC at higher temperatures to form certain volatile C-containing species. In this experiment, the products were stable in a vacuum condition. Note that the unwanted η phases (CCo_2W_4 and W_2C) generated at lower temperatures could not be eliminated by prolonging the holding time or increasing the temperature, but were inhibited when the reaction temperature was directly rised to 950 °C.

The SEM micrograph of WC—VC—Co composite powders prepared at 950 °C for 1 h is illustrated in Fig. 4. The powders exhibited spherical morphologies with a uniform size distribution, and the particle sizes ranged from 40 nm to 60 nm.

In conventional production processes of coarse-grain WC—VC—Co composite powders, the carburization temperature ranges from 1400 °C to 1600 °C, and the milling times may require up to 10+ h to homogeneously mix the starting powders [22,23]. In our experiment, the results clearly indicated that the required carburization temperature to fully convert the precursor to WC—VC—Co is much lower than that in conventional processes, and the experiment requires no milling for the mixing process. Given that the elements W, Co, V and C are tightly mixed, C can easily reduce the metal compounds and carburize with W and V in short-distance diffusion. As a result, the reaction temperature is low and the reaction time is short. The low temperature enables the formation of the WC nanostructures while grain growth is

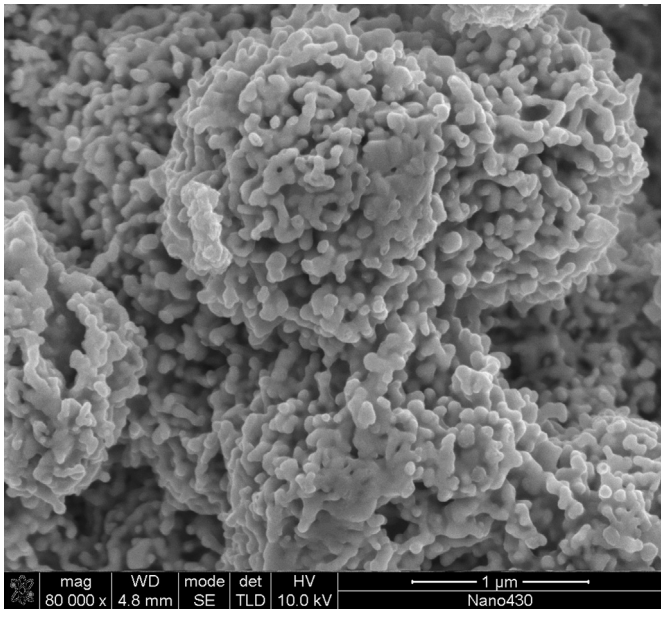

Fig. 4. SEM image of the samples prepared at 950 °C, 1 h.

significantly inhibited. Hence, the whole reaction is completed at a relatively low temperature and in a short time period.

X-ray photoelectron spectroscopy (XPS) was performed on WC—VC—Co sample obtained at 950 °C for 1 h (Figs. 5 and 6) to determine the elemental composition and binding state. The surface of a random sample consisted of W, Co, V, C, and O elements, which suggests that the components have a uniform distribution (Fig. 5). In Fig. 6a, the W 4f region displays four peaks at 37.47, 35.21, 33.62, and 31.36 eV. The two latter peaks are assigned to WC, and the two former are assigned to WO_3. WO_3 may have been generated when the thermodynamically unstable WC was slightly oxidized in air. The W, W_2C, and CCo_2W_4 peaks cannot be observed in Fig. 6a, which agrees with the XRD result in Fig. 3d. In Fig. 6b, an XPS spectrum of Co 2p region shows peaks at 800.76, 794.18, 784.05 and 778.2 eV. The peaks of 778.2 and 794.18 eV are assigned to Co, whereas the other two peaks are assigned to CoO. The peaks in the spectrum for the V 2p region (Fig. 6c) are observed at 524.3, 516.8 and 513.4 eV. The first two peaks are assigned to V2p3/2 and to V2p1/2 of V_2O_5, correspondingly, whereas the last peak corresponds to V_8C_7. In Fig. 6d, a typical XPS spectrum of O 1s energy region contains two deconvoluted peaks at 532.8 and 531.2 eV. The first peak is attributed to hydroxyl oxygen (OH^-) that mainly originated from air. OH^- can be removed by drying the sample at a certain temperature. The latter peak is at O 1s binding energy of M_xO_y (M = elements W, Co and V). The C 1s region (Fig. 6e) comprises two peaks at 284.5 (Cf) and 282.3 (Cc) eV. The Cc peak is due to the photoelectrons ejected from the C atoms in the WC. The Cf peak corresponds to the free C atoms contaminated on the sample surface and the excess of residual C in the reaction system. These results are in accordance with previous reported findings [24,25].

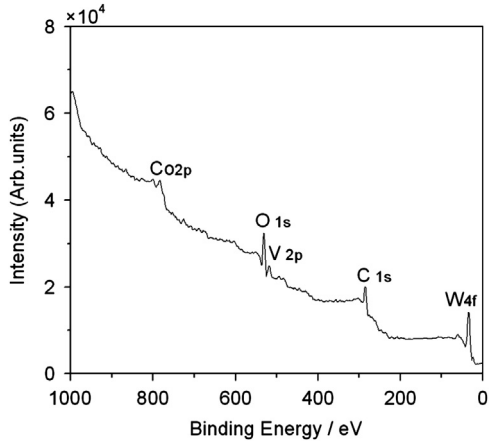

Fig. 5. XPS spectrum of WC—VC—Co nanocomposite powders.

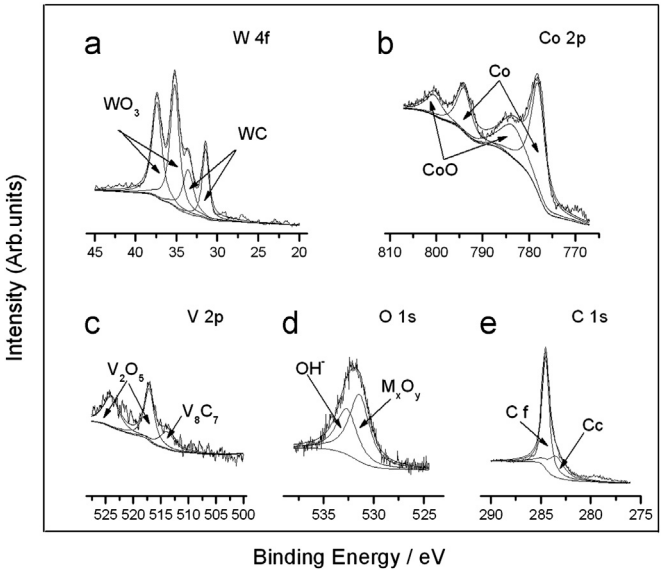

Fig. 6. XPS spectra of W 2f (a), Co 2p (b), O 1s (c) and C 1s (d) energy peaks for WC—VC—Co nanocomposite powders.

4. Conclusions

WC—VC—Co nanocomposite powders are successfully synthesized in vacuum via in-situ reduction and carburization of a novel core—shell precursor that was prepared using a hydrothermal route. The as-prepared powders have a narrow particle size distribution in the range of 40—60 nm. The optimal processing condition is under 950 °C for 1 h. The proportion of WC—VC—Co can be easily adjusted during preparation. This method offers a promising and cost-effective approach for the large-scale fabrication of WC—VC—Co nanocomposite powders and provides an opportunity to obtain high-performance cemented carbides.

Acknowledgments

This work was supported by the Fundamental Research Funds for the Central Universities (No. XDJK2010C009) and Chongqing Key Natural Science Foundation (cstc2012jjB50011).

References

[1] P. Ettmayer, Hardmetals and cermets, Annual Review of Materials Science 19 (1989) 145–164.
[2] R. Koc, S.K. Kodambaka, Tungsten carbide (WC) synthesis from novel precursors, Journal of the European Ceramic Society 20 (2000) 1859–1869.
[3] H.C. Kim, I.J. Shon, J.K. Yoon, S.K. Lee, Z.A. Munir, One step synthesis and densification of ultra-fine WC by high-frequency induction combustion, International Journal of Refractory Metals and Hard Materials 24 (2006) 202–209.
[4] S.F. Moustafa, Z.A. Hamid, O.G. Baheig, A. Hussien, Synthesis of WC hard materials using coated powders, Advanced Powder Technology 22 (2011) 596–601.
[5] M.F. Zawrah, Synthesis and characterization of WC—Co nanocomposites by novel chemical method, Ceramics International 33 (2007) 155–161.
[6] K. Jia, T.E. Fischer, B. Gallois, Microstructure, hardness and toughness of nanostructured and conventional WC—Co composites, Nanostructured Materials 10 (1998) 875–891.
[7] S.I. Cha, S.H. Hong, G.H. Ha, B.K. Kim, Microstructure and mechanical properties of nanocrystalline WC—10Co cemented carbides, Scripta Materialia 44 (2001) 1535–1539.

[8] Z.G. Ban, L.L. Shaw, Synthesis and processing of nanostructured WC—Co materials, Journal of Materials Science 37 (2002) 3397–3403.
[9] B.H. Kear, L.E. McCandlish, Chemical processing and properties of nanostructured WC—Co materials, Nanostructured Materials 3 (1993) 19–30.
[10] F.L. Zhang, C.Y. Wang, M. Zhu, Nanostructured WC/Co composite powder prepared by high energy ball milling, Scripta Materialia 49 (2003) 1123–1128.
[11] Z.Y. Zhang, S. Wahlberg, M.S. Wang, M. Muhammed, Processing of nanostructured WC—Co powder from precursor obtained by co-precipitation, Nanostructured Materials 12 (1999) 163–166.
[12] V. Bonache, M.D. Salvador, V.G. Rocha, A. Borrell, Microstructural control of ultrafine and nanocrystalline WC—12Co—VC/Cr_3C_2 mixture by spark plasma sintering, Ceramics International 37 (2011) 1139–1142.
[13] R. Polini, F. Bravi, G. Mattei, G. Marcheselli, E. Traversa, Effect of WC grain growth inhibitors on the adhesion of chemical vapor deposition diamond films on WC—Co cemented carbide, Diamond and Related Materials 11 (2001) 242–248.
[14] B.K. Kim, G.H. Ha, G.G. Lee, D.W. Lee, Structure and properties of nanophase WC/Co/VC/TaC hardmetal, Nanostructured Materials 9 (1997) 233–236.
[15] K. Bonny, P.D. Baets, J. Vleugels, S. Huang, O.V. Biest, B. Lauwers, Impact of Cr_3C_2/VC addition on the dry sliding friction and wear response of WC—Co cemented carbides, Wear 267 (2009) 1642–1652.
[16] K. Choi, N.M. Hwang, D.Y. Kim, Effect of VC addition on microstructural evolution of WC—Co alloy: mechanism of grain growth inhibition, Powder Metallurgy 43 (2000) 168–172.
[17] H.R. Lee, D.J. Kim, Role of vanadium carbide additive during sintering of WC—Co: mechanism of grain growth inhibition, Journal of the American Ceramic Society, 86, 152–154.
[18] L. Sun, T.E. Yang, C.C. Jia, J. Xiong, VC, Cr_3C_2 doped ultrafine WC—Co cemented carbides prepared by spark plasma sintering, International Journal of Refractory Metals and Hard Materials 29 (2011) 147–152.
[19] S.G. Huang, L. Li, O.V. Biest, J. Vleugels, VC- and Cr_3C_2-doped WC—NbC—Co hardmetals, Journal of Alloys and Compounds 464 (2008) 205–211.
[20] H. Lin, B.W. Tao, Q. Li, Y.R. Li, In situ synthesis of WC—Co nanocomposite powder via core—shell structure formation, Materials Research Bulletin 47 (2012) 3283–3286.
[21] S. Supothina, P. Seeharaj, S. Yoriya, M. Sriyudthsak, Synthesis of tungsten oxide nanoparticles by acid precipitation method, Ceramics International 33 (2007) 931–936.
[22] S. Yih, C. Wang, Tungsten: Source, Metallurgy, Properties and Applications, Plenum Press, New York, 1979.
[23] DH. Jack, Cemented carbide as an engineering material, in: M.M. Schwartz (Ed.), Engineering Application of Ceramic Materials: Source Book, American Society for Metals, Materials Park, OH, 1985, pp. 147–153.
[24] B.Z. Michael, J.G. Chen, Synthesis, characterization and surface reactivity of tungsten carbide (WC) PVD films, Surface Science 569 (2004) 89–98.
[25] E. Cappelli, S. Orlando, F. Pinzari, A. Napoli, S. Kaciulis, WC—Co cutting tool surface modifications induced by pulsed laser treatment, Applied Surface Science 138—139 (1999) 376–382.